Laser and Particle Beams (2000), *18*, 307–313. Printed in the USA.

The implosion dynamics and emission characteristics of Al liner-on-wire implosions

R. ROSCH,[1] D. FRIART,[1] M. DARRIGOL,[1] L. CHATRIEUX,[1] P. ZEHNTER,[1]
P. ROMARY,[2] AND J.M. CHEVALIER[2]
[1]CEA-BP 12-91680 Bruyères-le-Châtel
[2]CEA CESTA-BP 2-91680 Le Barp.

(RECEIVED 30 November 1998; ACCEPTED 14 October 1999)

Abstract

Previous experiments at 0.1 TW level have shown that stability and X-ray emission of fast *Z*-pinch could be significantly improved by imploding an Al vapor jet onto a very thin coaxial wire (Wessel *et al.*, 1992). Here we present the first results of an Al *Z*-pinch using a similar liner but at mega-ampere level. The pinch is driven by AMBIORIX facility, a 2 TW, 0.5 Ω, 2 MA, and a 50-ns pulse-line generator. We study the effect of an Al wire and its diameter (20–50 μm) on the implosion dynamics, on X-ray yield, on-axis magnetohydrodynamics (MHD) stability, and on Rayleigh–Taylor instability of the column at stagnation. Analysis of an Al jet on Al wire shots demonstrates that X-ray yield due to emission processes in the H- and He-like ionization stages (i.e., the *K*-shell) is enhanced, relative to the ones with Al jet only. The wire leads also to a better symmetrization of the implosion, and to better reproducibility of the shots. X-ray signals exhibit two similar pulses, 10-ns-wide and separated by 15 ns. To discern spectrally the origin of each pulse, further experiments have been performed with stainless steel wire (25 μm in diameter). Results show that liner and wire radiate simultaneously and contribute to both pulses. Full analysis of a typical Al jet on Al wire shot, using detailed collisional-radiative equilibrium (CRE) model is given in this paper. A sketch of the pinch at stagnation, with a cold dense core embedded in a hot low density corona, reproduces well all features of X-ray emission.

1. INTRODUCTION

Over 40 years, many research have been lead to achieve stability and homogeneity in high-density, high-temperature plasmas initiated from magnetically self-constricted discharges, when compared to the beginnings of fusion research with *Z*-pinches (Anderson *et al.*, 1958; Sethian, 1997). A fundamental approach was to start from a small diameter wire at high density, and keep it that way, as the current was increasing. Thus, many studies have been realized with cryogenic deuterium fibers (Chittenden *et al.*, 1997) for applications in thermonuclear fusion. The problem is that, despite the development of fast pulsed power technologies, until now, drivers still can not deliver energy into the wire fast enough to suppress its coronal expansion, hence, instability formation at recompression (Pereira & Davis, 1988; Lindemuth *et al.*, 1989). To reduce the energy deposition time, another approach proposed to use the intermediate conversion of electromagnetic energy into kinetic energy of an accelerated plasma shell (Bazilevskaya *et al.*, 1962). Experiments, such as the double liner or the plasma-on-wire configurations, considered fast collisions of accelerated liners onto targets. In the last scheme, the pulsed current is carried in a large diameter preformed liner, imploding onto a small diameter coaxial target. Coronal expansion from the target during jet implosion is thus limited, and so will be the development of MHD instabilities. Experiments on the GAEL high pulsed power generator (0.1 TW, 225 kA, 110 ns, and 2 Ω) have lead to a relatively homogeneous plasma radiation source, using an Al-annular jet (Anderson *et al.*, 1958; Gaziax *et al.*, 1984) as the outer liner. The work reported in this paper uses a similar configuration, but at a higher level. Other experiments, with neon puff liners imploding on high-*Z* wire targets were conducted on the Tandem puff generator (3.2 MA, 2 μs), by Wessel *et al.* (1997) and confirmed the enhancement of radiation yield using a target, compared to a pinch without a target.

Address correspondence and reprint requests to: Rudolf Rosch, 10, rue Toulouse Lautrec, 91300 Massy, France. E-mail: rudolf.rosch@wanadoo.fr

2. EXPERIMENTAL SET-UP

We have conducted experiments on AMBIORIX (Romary *et al.*, 1995; Gasque, 1996), a high pulsed power generating unit, based on the well-proven technology of Marx capaci-

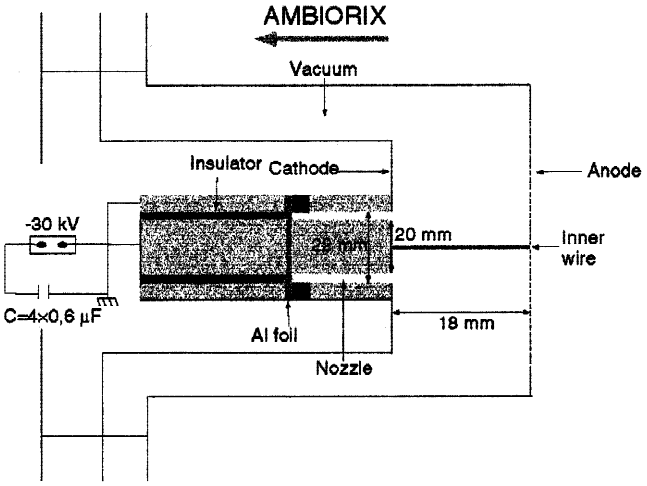

Fig. 1. Schematic of AMBIORIX load region showing the electrodes, Al wire, and Al plasma jet nozzle.

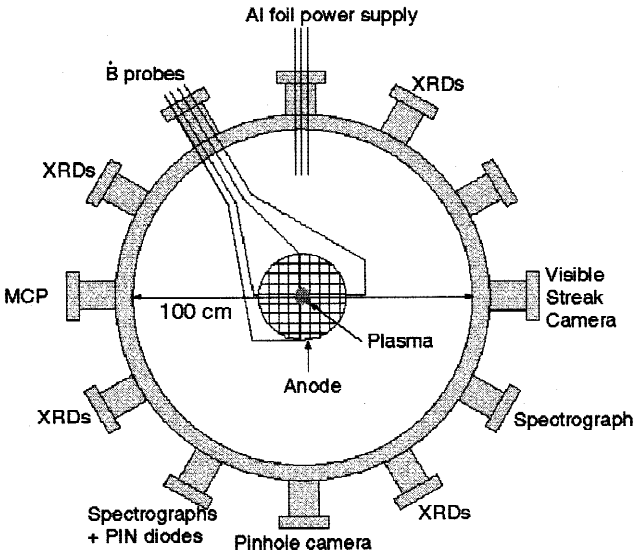

Fig. 2. View along the pinch axis of the arrangement of diagnostics and dB/dt probes on AMBIORIX.

tor banks. This Marx consists of forty eight 1.95 μF, 80 kV capacitors connected in a bipolar configuration, giving an output voltage of 3.8 MV and stored energy of 3000 kJ. It charges a transmission line, filled with water, which is then switched into the load (Fig. 1) where parameters are: 0.5 Ω, 1.2 MV, 2 MA, and 50 ns.

The load consists of an Al hollow plasma jet, with a mass-per-unit length of about 50 μg/cm, imploding on a Al wire (20-μm or 50-μm diameter). The jet is prepared by exploding a 3-μm-thick Al foil with an external capacitor bank (80 kA, 1 μs). The plasma jet forms a supersonic hollow plasma column (MACH 2) between the discharge electrodes, spaced by 18 mm apart. The jet is different from the one in GAEL experiments, where it was collimated by a 3-mm-diameter nozzle located in the anode. The mass-per-unit length in the plasma column is adjusted by varying the time delay between the firing of the generator and exploding the foil (Audebert *et al.*, 1990). Separate characterization of the jet was performed on a additional device, using Michelson and Mach–Zehnder resonant interferometry (Barnier *et al.*, 1998). Analysis of AI transition at 394.4 nm [$3s^2 3p$-$3s^2(^1S)4s$] and Al II transition at 466.3 nm [$3p^2$-$3s(^2S)4p$] have shown that most of the atoms in the jet are neutral.

3. DIAGNOSTICS

A wide set of diagnostics were implemented around the experimental chamber (Fig. 2). The implosion dynamics are studied with a visible streak camera. A 1-mm aperture slit, perpendicular to the pinch axis, images the center of the plasma. Two convex curved-crystal spectrographs (RbAp, Mica) collect the X-ray spectra. Data are recorded onto Kodak DEF X-ray film. The spectra are scanned with a digitizing Joyce scanning densitometer. Film densities are recorded every 10 μm across the film using a 20-μm-wide densitometer slit. In this paper, the spectral data are reported as intensities relative to the X-ray emission incident on the X-ray crystals.

Three KAP flat-crystal optics are coupled with three silicon PIN-type diodes to record time-resolved spectra of Al: the He-like triplet He(1s2p-$1s^2$), the H-like singlet H(1s-2s), and the He-like singlet He(1s-3s). Signals are spatially integrated.

An X-ray pinhole camera consisting of three apertures of size 50 μm records the plasma image on a DEF film, using various filters (10 μm Al, 10 μm Be, 5 μm Ti) to cover the 700 eV–5 keV energy range. X-ray snapshots are obtained using a SLIX intensified microchannel camera (Wiza, 1979; Kilkenny, 1991). Twenty-four images are projected by a 24 pinhole array on the eight microstrips of the detector. Time resolution is 1 ns and spatial resolution is 300 μm.

The XRD array consists of six photoelectric diodes, filtered with 15 μm and 30 μm C-Cl, 30 μm C-Cl, 16 μm Mg, 7 μm Al, 2.5 μm Zn, and 5 μm Ti. Filters have been chosen in order to determine spectrum for energies ranging from 700 eV to 5 keV (Fig. 3). Three PIN diodes, filtered with 10 μm Ag, 50 μm Ti, and 40 μm Zn (sensitivity curves not represented), measure hard X-ray emission (2–10 keV). All detectors have been calibrated such that signals can be considered accurate within 20%. Signals are spatially integrated.

4. RESULTS

Experiments on AMBIORIX consisted of approximately 40 shots. In this section, we will present the X-ray measurements from Al liner and then Al liner-on-Al wire implosions. To verify that the energy coupling from the generator is similar between puff-on-wire and puff only implosions, we compare the measured currents in Figure 4. Variations in amplitude are only due to reproducibility of shots. The cur-

https://doi.org/10.1017/S0263034600182217 Published online by Cambridge University Press

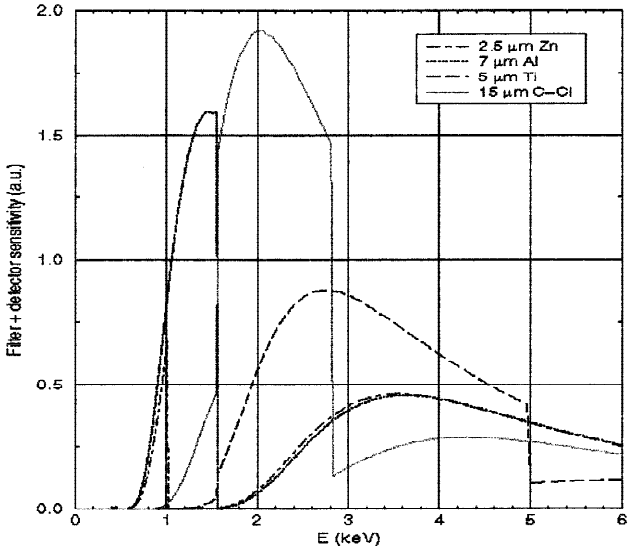

Fig. 3. Sensitivity curves for XRD filters.

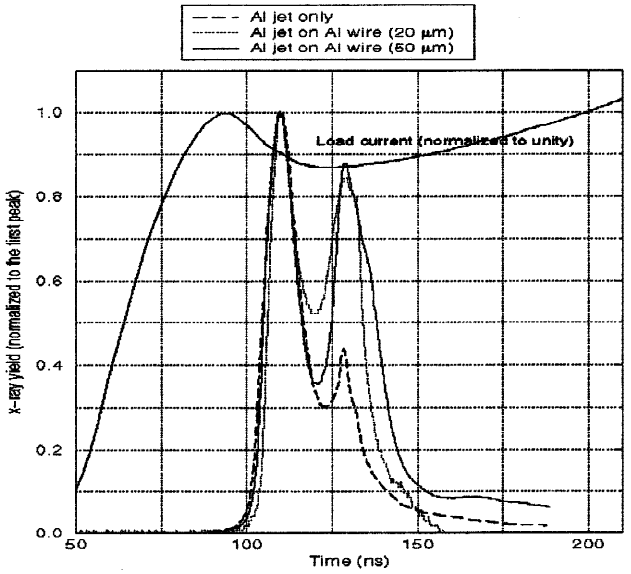

Fig. 5. *K*-shell radiation as measured by XRDs, for Al jet only (shot # 1047) and Al jet on Al wire configurations [shot # 1046 (20 μm) and shot # 1041 (50 μm)].

rent pulse begins with a 30 ns prepulse followed by the main pulse rising in 50 ns. The current in the load is integrated by a *B*-dot probe and is expected to be reliable only during the first 80 ns of the main discharge. After, current probes are screened by expanded plasma and linear growth of signals are due to numerical integration of a nonphysical constant.

Data from the X-ray diodes can be seen in Figure 5 and Figure 6, for Al jet only and Al jet on Al wire configurations. The first peaks of the signals have been normalized to unity, in order to compare the pulse characteristics of all channels. Figure 5 displays pulses corresponding to *K*-shell radiation, obtained by carbon-chlorine filtered detectors (1.5–2.6 keV transmission band, see Fig. 3). The Al jet only signal exhibits a first pulse, 10 to 15 ns wide, then a second one, 20 ns afterwards, 2–3 times smaller and a few nanoseconds longer. Energy radiated in Al *K*-shell is approximately 500 J, with a great dispersion from shot-to-shot (Table 1). Al jet on Al wire signals present a different behavior: two similar pulses, separated by 20 ns. No dependence is observed with wire diameter. Radiated energy in *K*-shell is about 1 kJ. A good reproducibility is obtained, with shot-to-shot variations less than 20%.

Figure 6 represents X-ray detectors (XRD) signals filtered with Mylar (large-band filter). All pulses behave similarly to *K*-shell radiation signals, but with additional low

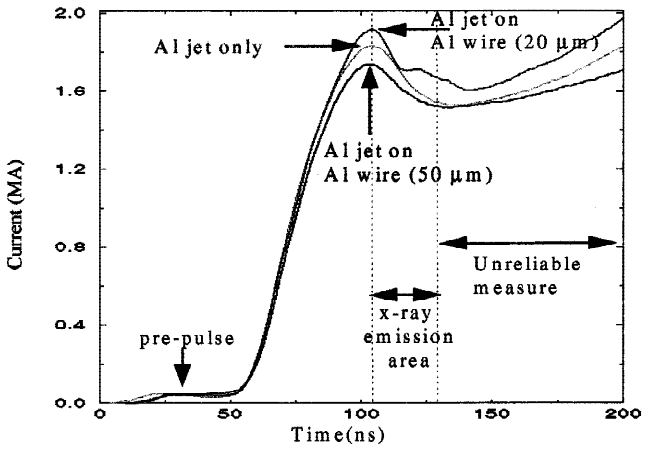

Fig. 4. Typical load current signals, for Al liner only and Al liner on Al wire configurations.

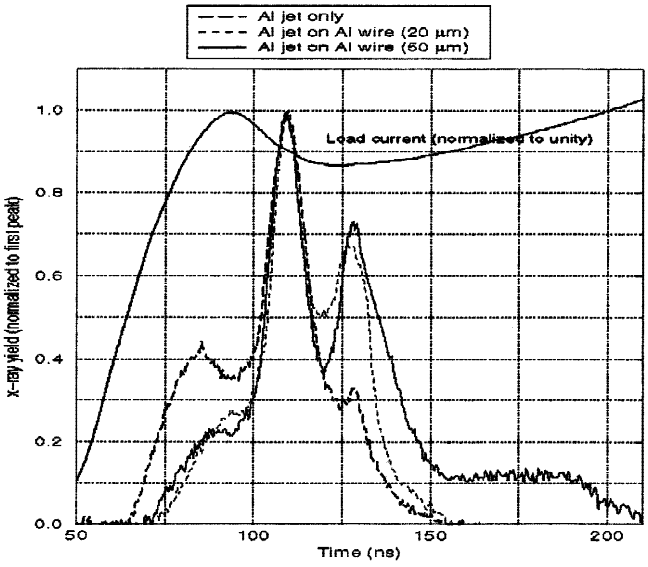

Fig. 6. *K*-shell + low energy radiation as measured by XRDs, for Al jet only (shot # 1047) and Al jet on Al wire configurations [shot # 1046 (20 μm) and shot # 1041 (50 μm)].

https://doi.org/10.1017/S0263034600182217 Published online by Cambridge University Press

Table 1. *Basic data from typical Al jet only and Al jet on Al wire shots on AMBIORIX*

Shot #	Central wire	Load current (MA)	Implosion time (ns)*	Pulse width (ns)	*K*-shell yield (J)	*K*-shell power (GW) at first peak
1001	no wire	2.10	77 (1 peak)	11	350	27
1010	no wire	1.70	67 (1 peak)	14	720	50
1038	Al (20 μm)	1.76	54–68 (2 peaks)	24	735	19
1046	Al (20 μm)	1.85	63–82 (2 peaks)	28	836	19
1036	Al (50 μm)	1.78	63–75 (2 peaks)	23	1004	23
1041	Al (50 μm)	1.82	66–85 (2 peaks)	30	809	17

*Implosion time is the delay between main current rise and X-ray emission.

energy emission (about 50-ns wide). No significant variation of *K*-shell radiation with the wire diameter (20–50 μm) is seen. This remark suggests that a similar mass of the wire (approximately 8 μg/cm, that is the 20 μm diameter wire) participates to radiation in both cases. In the 50 μm case, the internal core is heated to a lower temperature, and radiates soft energy photons. This low energy emission appears on the long lasting signal in Figure 6.

After these experiments, we thought that the first pulse was due to liner and that second one to wire. Therefore, we decided to separate spectrally emissions of liner and wire, by changing the wire material. Stainless steel (composition is 72% Fe, 10% Ni, 8% Cr) was chosen in these experiments, because it radiates between 900 eV and 1500 eV for *L*-shell and above 5 keV for *K*-shell, so that previous filterings could be maintained. XRDs filtered with chlorine are used for *K*-shell liner emission, and XRDs filtered with Al for *L*-shell wire emission. PIN detectors filtered with Ag (2–3 keV), Ti (3–5 keV), Zn (5–8 keV) give information on hard X-ray radiation, and especially *K*-shell emission of stainless steel (above 5 keV). Time-resolved signals shown in Figure 7 prove that liner and wire radiate simultaneously, and contribute together to both X-ray pulses. The analysis of PIN diode signals (not presented here) shows that radiation around 5 keV is significantly enhanced in the presence of the stainless steel wire.

Implosion dynamics (Fig. 8) appears independent of the presence of the wire. Al jet only and Al jet on Al wire configurations show an 11-mm radius liner (nozzle radius) 20 ns before stagnation, where the radius is approximately 2–3 mm. In the presence of wire, significant visible light appears on the axis about 10 ns before implosion and indicates that the wire is heated prior to the outer liner implosion. This heating may be explained by two effects: a small fraction of current passing through the wire and outer liner radiation. Double stagnation observed in X-ray signals is indicated on images. As noticed on X-ray signals, low-energy radiation stops after the second pulse in the 20 μm case, but keeps on for more than 50 ns in the 50 μm case.

Figure 9 displays plasma snapshots obtained with a strip line imager X (SLIX) detector, coupled with a coupled charge device (CCD) camera. Figure 9a shows that Al jet only pinch at the time of stagnation, and 18 ns later. The plasma appears inhomogeneous with no more integrity, and gaps in the axial emissions. In the Al jet on Al 20-μm-diameter wire (Fig. 9b), the wire appears twisted and mixed to the outer plasma. Fig. 9c demonstrates the good homogeneity of the pinch obtained with a 50-μm-diameter wire at first stagnation. After this first stagnation, studies of snapshots (not given here) show the evolution of a highly compressed plasma near the anode, that modifies nonuniformly the shell profile. This appears to be a sausage mode from MHD or Rayleigh–Taylor instability.

The next section is dedicated to the determination of the stagnated plasma parameters, that is temperature and density. This analysis needs the pinch to be relatively homogeneous, because our experimental data are integrated in space. Therefore, we will study the Al jet on an Al 50 μm configuration (shot # 1041).

4.1. Analysis of an Al jet on an Al 50 μm wire shot (# 1041)

The principal tool which we have used to analyze the extensive X-ray data collected from these experiments and to determine plasma temperature and density at first stagnation

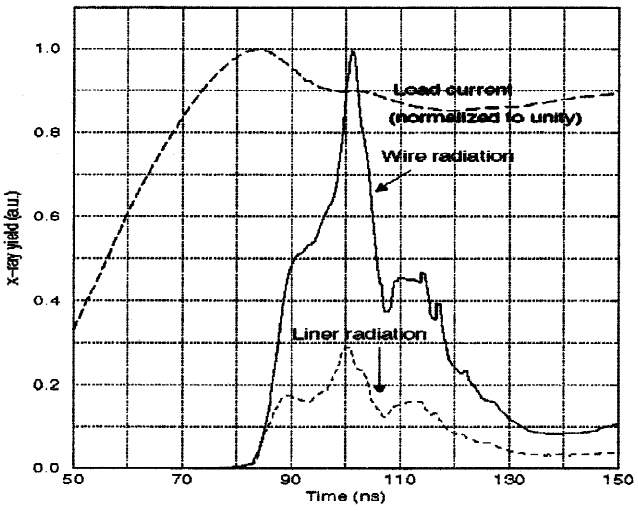

Fig. 7. X-ray pulses as measured by XRDs for the Al jet on stainless steel wire (25 μm in diameter) configuration (shot # 1043).

https://doi.org/10.1017/S0263034600182217 Published online by Cambridge University Press

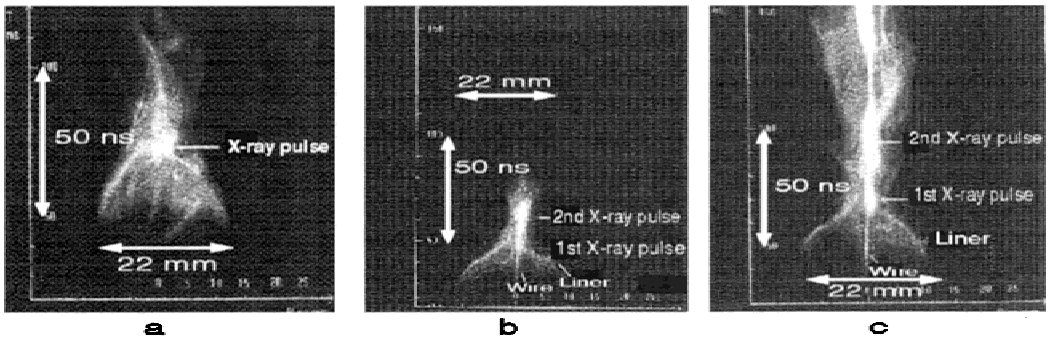

Fig. 8. Implosion dynamics (time *vs.* radius) as seen with a visible streak camera, (a) for the Al jet only (shot # 1047), (b) for the Al jet on Al wire (20 μm) (shot # 1046), (c) for the Al jet on Al wire (50 μm) (shot # 1041).

is a 1D, collisional-radiative-equilibrium (CRE) model (Lee *et al.*, 1984). The atomic level structures contained in this model include all the ground states of the various ionization stages as well as a variety of excited states from Al XI to Al XIII. Most of the detailed structure is contained in the *K*-shell. Populations are calculated from rate equations including relevant collisional and radiative processes. The code produces line ratio and synthetic spectra for any arbitrary density and temperature. For the calculations presented here, the plasma is taken as a homogeneous cylindrical column of uniform density and temperature.

Figure 10 shows a spectral region containing the He- and H-like resonance lines in Al XI and Al XII. This spectrum was obtained with the time- and space-integrated spectrograph. Using the CRE model, reconstitution of this spectrum is possible if we consider two emissive areas: a central media surrounded by a corona. More precisely, a 500-μm-diameter core at a density of 3×10^{20} cm^{-3} and at temperature of 350 eV produces the He-like lines. In these conditions, the 1s2p-1s^2(^{1}P) resonance line is optically thick. A 3-mm-thick coronal plasma, at electronic temperature of 900 eV and electronic density of 3×10^{19} cm^{-3} produces the H-like lines which are optically thin. Temperatures are determined using absolute intensity of lines. Densities are obtained with an iterative process: a theoretical (Ne, Te) spectrum is injected in a postprocessor, giving the output signal of an XRD. This signal is then compared to the experimental one. Variation on density is iterated until a good agreement is found between theoretical and experimental signals on all detectors. This method uses only absolute intensity of lines.

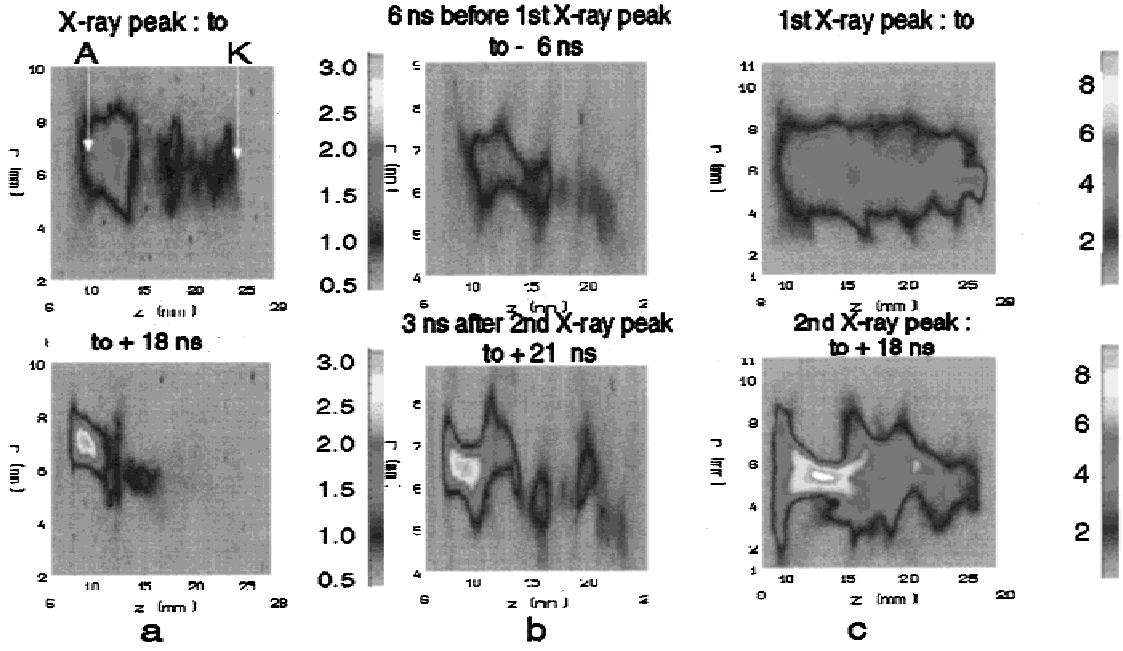

Fig. 9. *K*-shell radiation 1-ns snapshots (radius *vs.* pinch axis) of the pinch, at the time of stagnation for the Al jet only (a, shot # 1047), for the Al jet on Al 50-μm-diameter wire (c, shot # 1041), and near stagnation for the Al jet on Al 20-μm-diameter wire (b, shot # 1046). The left color scale refers to (a), the right one refers to (b) and (c).

https://doi.org/10.1017/S0263034600182217 Published online by Cambridge University Press

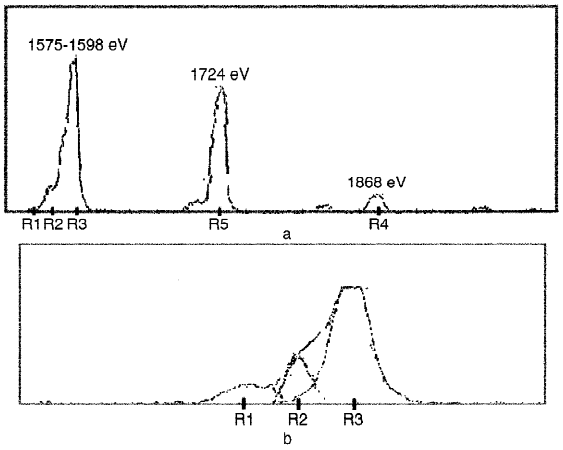

Fig. 10. Time- and space-integrated spectrum of shot No. 1041 (Al jet on Al 50-μm-wire), showing (a), the H (at 1724 eV)- and He-like Al (1575–1598 eV and 1868 eV) and (b), a detailed view of the He-like triplet between 1575 eV and 1598 eV.

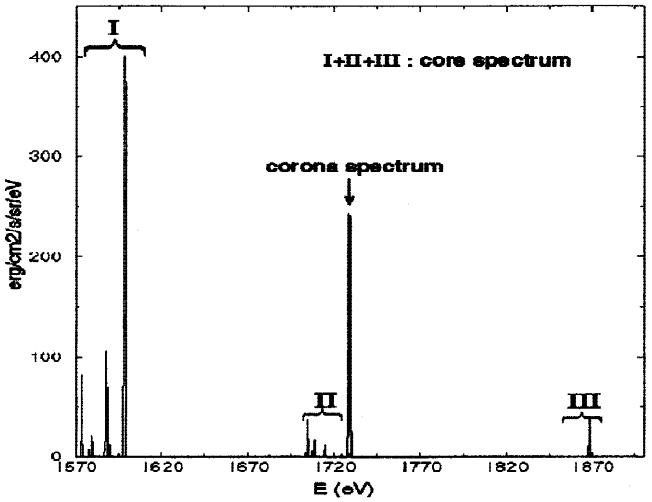

Fig. 11. Theoretical spectrum of the pinch at first stagnation (shot # 1041), using the CRE model.

Line ratio method is inadequate because lines are emitted from different regions, and thus cannot be compared. Figure 11 shows the theoretical spectrum we have obtained with these conditions.

We have to note, that a work by Apruzese *et al*. (1998), demonstrated that different temperature profiles could be ruled out by the small amount of data which usually can be recorded accurately. Therefore, we found some parameters that fit experimental results, but there might be other solutions.

The electronic temperature found for the internal part of the pinch may be confirmed by a method based on the analysis of the optically thick He-like resonance line (1598 eV). Planck law gives the intensity of a thick line (B_υ) as a function of brightness temperature (T_b),

$$B_\upsilon(T_\upsilon) = \frac{2h\upsilon^3}{c^2}\,\frac{1}{\exp\left(\dfrac{h\upsilon}{kT_b}\right)-1}. \qquad (1)$$

Brightness temperature is a property of radiation which differs from electronic temperature in our pinch, because the plasma is in nonlocal thermodynamic equilibrium. Using the CRE model, we can calculate brightness temperature (at first B_υ, by integrating the intensity of the thick line, then T_b) as a function of electronic temperature and density. Results are presented in Figure 12.

We note that, for electronic densities from 1 to 5 $\times$ 10^{20} cm^{-3}, brightness temperature depends slightly on electronic temperature. If we suppose the density to be within this range (density was estimated to 3 $\times$ 10^{20} cm^{-3} previously), integration of the He-like line on the previous experimental spectrum gives a brightness temperature of approximately 220 eV, which corresponds to an electronic temperature (averaged on *Z*-pinch size) of 350 eV. The synthetic view of the pinch at stagnation is given in Figure 13.

5. CONCLUSION

We have performed Al-pinch on Al-wire experiments on AMBIORIX facility, a 2 TW, 0.5 Ω, 2 MA, 50 ns pulse-line generator. Comparison of the behavior of the Al plasma jet at MA level, with and without coaxial Al wire (20–50 μm diameter) suggests some characteristics in the presence of the wire: enhanced power in the multi keV range, a multipeak, radiation pulse structure, a relatively homogeneous

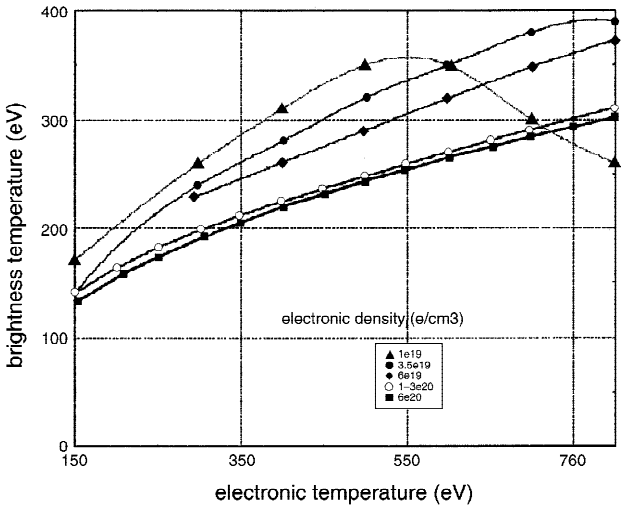

Fig. 12. Brightness temperature (eV) as a function of electronic temperature and density.

https://doi.org/10.1017/S0263034600182217 Published online by Cambridge University Press

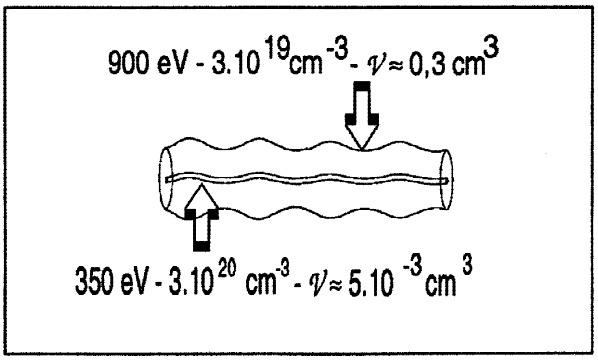

Fig. 13. Plasma parameters of a Al jet on an Al 50-μm wire diameter, at first stagnation (shot No. 1041).

pinch at first stagnation, with a 50-μm-diameter wire. We have observed that the current rise in the load does not depend on the presence of the wire, at least prior to the time of maximum compression (after, the measure is no more reliable). Images by streak camera suggest that the implosion of the Al plasma jet appears unaffected by the presence of a wire at its core. To explain the two-peak form observed in X-ray signals, we realized experiments with a stainless steel wire (25-μm-diameter). Results showed that the liner and the wire radiate simultaneously and both contribute to each pulse.

Using a CRE model, a spectroscopic analysis based on absolute radiation signals has shown that an Al jet on an Al wire implosion can be described at the stagnation as a composite structure. The pinch consists of a cold-dense core (350 eV, 3×10^{20} cm^{-3}), embedded in a hot-low density corona (900 eV, 3×10^{19} cm^{-3}). This analysis reproduces all features of the observed data.

ACKNOWLEDGMENTS

The authors are grateful to the AMBIORIX operations crew for their proficient technical support during the experiments. In addition, we would like to address a special thank to G. de Lacheze Murel, for his support and help in plasma simulations and to Dr. Jean Larour, of *Laboratoire de Physique des Milieux Ionisés* (École Polytechnique, France), for his constant assistance, suggestions and comments on this work.

REFERENCES

Anderson, O.A., Baker, W.R., Colgate, S.A., Ise, J. & Ryle, R.V. (1958). *Physical Review* **110**, 24.

Apruzese, J.P., Thornhill, J.W. & Whitney, K.G. *et al.* (1998). In *IEEE Transactions of Plasma Science* **26**, 1185.

Audebert, P., Lamain, H., Dufour, B., Rouille, C., Etlicher, B., Voisin, L. & Romary, P. (1990). In *Proc. of the Eighth Int. Conf. on High Power Particle Beams* (Novosibirsk) (Brelzman, B., and Knyazev, B., Eds.), Vol. 1, p. 422. Singapore: World Scientific.

Barnier, J.N., Chevalier, J.M., Dubroca, B. & Rouch, J. (1998). In *IEEE Transactions on Plasma Science, Special Edition on Z-Pinches* **6**, 229.

Bazilevskaya, O.A., Andrianov, A.M., Demichev, V.F. & Vasiljev, V.I. (1962). In *Proc. of the Fifth Int. Conf. on Ionization Phenomena in Gases*, Amsterdam.

Chittenden, J.P., Aliaga Rossel, R.F., Lebedev, S.V., Mitchell, I.H., Bell, A.R., Beg, F.N., Lorenz, A., Dangor, A.E., Haines, M.G. & Decker, A. (1997). In *Proc. of the Fourth Int. Conf. on Dense Z-Pinches*, Vancouver.

Gasque, A.M., Romary, P., Dan'ko, S. & Gorbulin, Y. *et al.* (1996). In *Proc. of the Eleventh Int. Conf. on High Power Particle Beams*, Prague.

Gazaix, M., Doucet, H.J., Etlicher, B., Furtlehner, J.P., Lamain, H. & Rouille, C. (1984). *J. Appl. Phys.* **56**, 3209.

Kilkenny, J.D. (1991). *Laser Particle Beams* **9**, 49.

Lee, R.W., Whitten, B.L. & Stout, R.E. (1984). *J. Quant. Spect. Radiat. Transfer* **32**, 91.

Lindemuth, I., McCall, G.H. & Nebel, R.A. (1989). *Phys. Rev. Lett.* **62**, 264.

Pereira, N.R. & Davis, J. (1988). *J. Appl. Phys.* **64**, R21.

Romary, P., Eyl, P. & Angles, J.M. (1995). In *Proc. of the Tenth Pulsed Power Conf.*, p. 1074.

Sethian, J. (1997). In *Proc. of the Fourth Int. Conf. on Dense Z-Pinches*, Vancouver.

Smirnov, V.P. (1991). *Plasma Phys. Controlled Fusion* **33**, 1697.

Wessel, F.J., Coleman, P.L., Loter, N., Ney, P., Rahman, H.U., Rauch, J. & Thompson, J. (1997). *J. Appl. Phys.* **81**, 3410.

Wessel, F.J., Etlicher, B. & Choi, P. (1992). *Phys. Rev. Lett.* **69**, 3181.

Wiza, J.L. (1979). *Nuclear Instruments and Methods* **162**, 587.